BRIEF COMMUNICATIONS

The purpose of this Brief Communications section is to present important research results of more limited scope than regular articles appearing in Physics of Fluids. Submission of material of a peripheral or cursory nature is strongly discouraged. Brief Communications cannot exceed four printed pages in length, including space allowed for title, figures, tables, references, and an abstract limited to about 100 words.

An extrapolation method for boundary conditions in lattice Boltzmann method

Zhaoli Guo[a] and Chuguang Zheng
National Laboratory of Coal Combustion, Huazhong University of Science and Technology, Wuhan 430074, China

Baochang Shi
Department of Mathematics, Huazhong University of Science and Technology, Wuhan 430074, China

(Received 7 June 2001; accepted 1 March 2002; published 6 May 2002)

A boundary treatment for curved walls in lattice Boltzmann method is proposed. The distribution function at a wall node who has a link across the physical boundary is decomposed into its equilibrium and nonequilibrium parts. The equilibrium part is then approximated with a fictitious one where the boundary condition is enforced, and the nonequilibrium part is approximated using a first-order extrapolation based on the nonequilibrium part of the distribution on the neighboring fluid node. Numerical results show that the present treatment is of second-order accuracy, and has well-behaved stability characteristics. © *2002 American Institute of Physics.*
[DOI: 10.1063/1.1471914]

The lattice Boltzmann method (LBM) has achieved great success in simulations of fluid flows and modeling physics in fluids.[1] In LBM, the boundary conditions influence the accuracy and stability of the computation. The usually used bounce-back scheme is easy for implementation and support the idea that LBM is ideal for simulating fluid flows in complicated geometries. However, the original bounce-back scheme is only of first order in numerical accuracy at boundaries,[2] and cannot be simply extended to handle moving boundaries or mass injection through the boundaries.[3] Some other boundary treatments have been proposed, such as the half-way bounce-back scheme,[4] the hydrodynamic approach,[3] the nonequilibrium bounce-back scheme,[5] and the extrapolation scheme,[6] and so on. These new approaches can yield improved results compared with the bounce-back scheme. However, they are most suitable for flat walls, and when used for curved walls, the boundaries must be represented by lattice nodes. As a result, the boundaries usually become jagged and will introduce some additional errors. Recently, an approach for curved walls was proposed by Fillipova and Hänel,[7] and was improved by Mei *et al.*[8]

In this paper we will propose an alternative treatment for curved walls in LBM. The basic idea is to decompose the distribution at a wall node into two parts, i.e., the equilibrium part and the nonequilibrium one. The nonequilibrium part is approximated by that of the neighboring fluid node along the link, and the equilibrium part is determined by a fictitious equilibrium distribution where the boundary condition is enforced.

For simplicity here we choose the two-dimensional (2D) square incompressible model (ID2Q9) proposed by He and Luo[9] to work. The evolution equation of ID2Q9 is

$$f_i(\mathbf{x}+\mathbf{e}_i\delta,t+\delta)-f_i(\mathbf{x},t)=-\tau^{-1}[f_i(\mathbf{x},t)-f_i^{(\mathrm{eq})}(\mathbf{x},t)], \tag{1}$$

where $\mathbf{e}_i$ are the particle velocities given by $\mathbf{e}_0=(0,0)$, $\mathbf{e}_i=(\cos(\pi(i-1)/2),\sin(\pi(i-1)/2))$ for $i=1-4$, and $\mathbf{e}_i=\sqrt{2}(\cos(\pi(i-9/2)/2),\sin(\pi(i-9/2)/2))$ for $i=5-8$. $f_i(\mathbf{x},t)$ is the distribution function for particles with velocity $\mathbf{e}_i$ at position $\mathbf{x}$ and time t, δ is the lattice spacing and the time increment in physical unit. τ is the dimensionless relaxation time, and $f_i^{(\mathrm{eq})}(\mathbf{x},t)$ is the equilibrium distribution function defined by

$$f_i^{(\mathrm{eq})}=\omega_i\left[\rho+\rho_0\left(\frac{\mathbf{e}_i\cdot\mathbf{u}}{c_s^2}+\frac{(\mathbf{e}_i\cdot\mathbf{u})^2}{2c_s^4}-\frac{\mathbf{u}^2}{2c_s^2}\right)\right], \tag{2}$$

where ω_i are weight coefficients given by $\omega_0=4/9$, $\omega_i=1/9$ for $i=1-4$, and $\omega_i=1/36$ for $i=5-8$. $c_s=1/\sqrt{3}$ is the sound speed of the model, ρ and $\mathbf{u}$ are the flow density and velocity given by $\rho=\Sigma_i f_i$, $\rho_0\mathbf{u}=\Sigma_i\mathbf{e}_i f_i$, where ρ_0 is the mean density. Through a Chapman–Enskog procedure, the incompressible Navier–Stokes equations can be derived from Eq. (1) with a shear viscosity $\nu=c_s^2\delta(\tau-0.5)$.

[a]Electronic mail: pcihust@public.wuhan.cngb.com

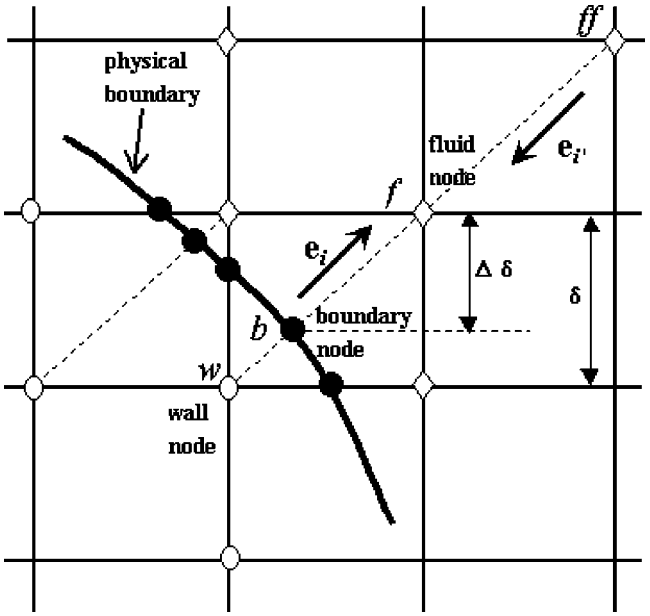

FIG. 1. Curved boundary and lattice nodes.

In evolution, the distribution functions at boundaries need to be specified according to boundary conditions for the macroscopic variables. Here we consider velocity boundary condition for curved walls. As shown in Fig. 1, the link between the fluid node $\mathbf{x}_f$ and the wall node $\mathbf{x}_w$ intersects the physical boundary at $\mathbf{x}_b$, and $\mathbf{x}_f=\mathbf{x}_w+\mathbf{e}_i\delta$. The fraction of the intersected link in the fluid region is $\Delta=(|\mathbf{x}_f-\mathbf{x}_b|)/(|\mathbf{x}_f-\mathbf{x}_w|)$.

Note that the evolution of ID2Q9 consists of two computational steps, i.e., the collision step $f_i^+(\mathbf{x},t)=f_i(\mathbf{x},t)-\tau^{-1}(f_i(\mathbf{x},t)-f_i^{(\mathrm{eq})}(\mathbf{x},t))$, and the streaming step, $f_i(\mathbf{x}+\mathbf{e}_i\delta,t+\delta)=f_i^+(\mathbf{x},t)$. Obviously, $f_i^+(\mathbf{x}_w)$ is needed to finish the streaming step for the fluid node $\mathbf{x}_f$. To specify $f_i^+(\mathbf{x}_w,t)$, just as usually done in the Chapman–Enskog procedure, we decompose $f_i(x_w,t)$ into two parts: $f_i(\mathbf{x}_w,t)=f_i^{(\mathrm{eq})}(x_w,t)+f_i^{(\mathrm{ne})}(\mathbf{x}_w,t)$, where $f_i^{(\mathrm{eq})}(\mathbf{x}_w,t)$ and $f_i^{(\mathrm{ne})}(\mathbf{x}_w,t)$ are the equilibrium and the nonequilibrium part of $f_i(\mathbf{x}_w,t)$, respectively. Instead of using the original definition Eq. (2), the equilibrium part is approximated by a fictitious one defined by

$$\overline{f}_i^{(\mathrm{eq})}(\mathbf{x}_w)=\omega_i\left[\overline{\rho}_w+\rho_0\left(\frac{\mathbf{e}_i\cdot\overline{\mathbf{u}}_w}{c_s^2}+\frac{(\mathbf{e}_i\cdot\overline{\mathbf{u}}_w)^2}{2c_s^4}-\frac{\overline{\mathbf{u}}_w^2}{2c_s^2}\right)\right], \tag{3}$$

where $\overline{\rho}_w\equiv\rho(\mathbf{x}_f)$ is an approximation of $\rho_w\equiv\rho(\mathbf{x}_w)$, and $\overline{\mathbf{u}}_w$ is an approximation of $\mathbf{u}_w=\mathbf{u}(\mathbf{x}_w)$ to be chosen. Note that the LBM can be viewed as a special finite-difference scheme for the Boltzmann equation on a discrete lattice.[10] Therefore, it is reasonable to determined $\overline{\mathbf{u}}_w$ by a linear extrapolation using either $\overline{\mathbf{u}}_w=\mathbf{u}_{w1}\equiv(\mathbf{u}_b+(\Delta-1)\mathbf{u}_f)/\Delta$ or $\overline{\mathbf{u}}_w=\mathbf{u}_{w2}\equiv(2\mathbf{u}_b+(\Delta-1)\mathbf{u}_{ff})/(1+\Delta)$, where $\mathbf{u}_f=\mathbf{u}(\mathbf{x}_f)$ and $\mathbf{u}_{ff}=\mathbf{u}(\mathbf{x}_{ff})$ with $\mathbf{x}_{ff}=\mathbf{x}_f+\mathbf{e}_i\delta$. Obviously, the difference between either $\mathbf{u}_{w1}$ or $\mathbf{u}_{w2}$ and $\mathbf{u}_w$ is $O(\delta^2)$. It is usually more accurate using $\mathbf{u}_{w1}$ than using $\mathbf{u}_{w2}$ to approximate $\overline{\mathbf{u}}_{wf}$ since $\mathbf{x}_f$ is closer to $\mathbf{x}_w$ than $\mathbf{x}_{ff}$. However, if Δ is small, the denominator in the expression of $\mathbf{u}_{w1}$ will be too large, and will lead to numerical instability in the computation. Therefore, we propose to use $\overline{\mathbf{u}}_w=\mathbf{u}_{w1}$ for $\Delta\geqslant 0.75$, and use a linear interpolation between $\mathbf{u}_{w1}$ and $\mathbf{u}_{w2}$ with weight Δ for $\Delta<0.75$, i.e., $\overline{\mathbf{u}}_w=\Delta\mathbf{u}_{w1}+(1-\Delta)\mathbf{u}_{w2}$. Either way gives that $\overline{\mathbf{u}}_w=\mathbf{u}_w+O(\delta^2)$.

It is well understood that in the incompressible limit, the density fluctuation is of order $O(M^2)$, where $M=u/c_s\ll 1$ is the Mach number. Therefore, $\overline{\rho}_w=\rho_w+\delta\mathbf{e}_i\cdot\nabla\rho=\rho_w+O(\delta M^2)$. Based on the expression of the shear viscosity υ, we can obtain that $M\approx u_0/c_s=c_s\mathrm{Re}(\tau-0.5)\delta/L$, where u_0 and L are the characteristic velocity and length, respectively, Re is the Reynolds number of the flow. Therefore, if τ is chosen such that $c_s\mathrm{Re}(\tau-0.5)/L=O(1)$, the Mach number M will be of the same order of the lattice spacing δ. We will concentrate on this case next. Based on these arguments, the difference between the fictitious equilibrium function $\overline{f}_i^{(\mathrm{eq})}(\mathbf{x}_w)$ and the original one $f_i^{(\mathrm{eq})}(\mathbf{x}_w)$ may be estimated that

$$\overline{f}_i^{(\mathrm{eq})}(\mathbf{x}_w)-f_i^{(\mathrm{eq})}(\mathbf{x}_w)=O(\delta^2). \tag{4}$$

The next task is to determine the nonequilibrium part $f_i^{(\mathrm{ne})}(\mathbf{x}_w,t)$. In the Chapman–Enskog analysis, $f_i^{(\mathrm{ne})}(\mathbf{x}_w,t)$ can be expressed as $f_i^{(\mathrm{ne})}=\delta f_i^{(1)}$, where $f_i^{(1)}$ is of the same order of $f_i^{(\mathrm{eq})}$. Note that $f_i^{(1)}(\mathbf{x}_w,t)-f_i^{(1)}(\mathbf{x}_f,t)=O(\delta)$, $f_i^{(1)}(\mathbf{x}_w,t)-f_i^{(1)}(\mathbf{x}_{ff},t)=O(\delta)$, thus $f_i^{(\mathrm{ne})}(\mathbf{x}_w,t)$ can be approximated by the nonequilibrium part of the distribution function at the fluid node $\mathbf{x}_f$ or $\mathbf{x}_{ff}$ with second-order accuracy. In order to be consistent with the definition of $\overline{\mathbf{u}}_w$, we propose to use $f_i^{(\mathrm{n})}(\mathbf{x}_w,t)=f_i^{(\mathrm{ne})}(\mathbf{x}_f,t)$ for $\Delta\geqslant 0.75$ and $f_i^{(\mathrm{ne})}(\mathbf{x}_w,t)=\Delta f_i^{(\mathrm{ne})}(\mathbf{x}_f,t)+(1-\Delta)f_i^{(\mathrm{ne})}(\mathbf{x}_{ff},t)$ for $\Delta<0.75$. Finally, we obtain the following boundary treatment to specify the post-collision distribution function $f_i^+(x_w,t)$,

$$f_i^+(\mathbf{x}_w,t)=\overline{f}_i^{(\mathrm{eq})}(\mathbf{x}_w,t)+(1-\tau^{-1})f_i^{(\mathrm{ne})}(\mathbf{x}_w,t). \tag{5}$$

We can conclude from the above discussions that the present boundary treatment is of second order accuracy in both time and space.

Note that the present treatment is different from the method proposed by Fillipova and Hänel[7] (refered to as FH) and the improved version proposed by Mei *et al.*[8] (referred to as MLS). First, the FH (MLS) treatments can be viewed as improvements of the bounce-back rule, but the present treatment is an extension of the extrapolation scheme by Chen *et al.*,[6] and shares the advantages such as the self-consistency and the easiness to be extended for other boundary conditions including a combination of density, velocity, temperature, and their derivatives. Second, the basic assumptions of the present and the FH (MLS) schemes are different. The FH (MLS) scheme is under the assumption that the flow is "slow," so they are only suitable for steady flows intrinsically. The basic requirement of the present scheme, however, is that the Mach number and the lattice spacing are of the same order. It is not a special condition for the present scheme in that this is usually a common requirement in LBM applications. Therefore, the present scheme needs no additional conditions in practice, and can be used for both steady and unsteady flow in theory.

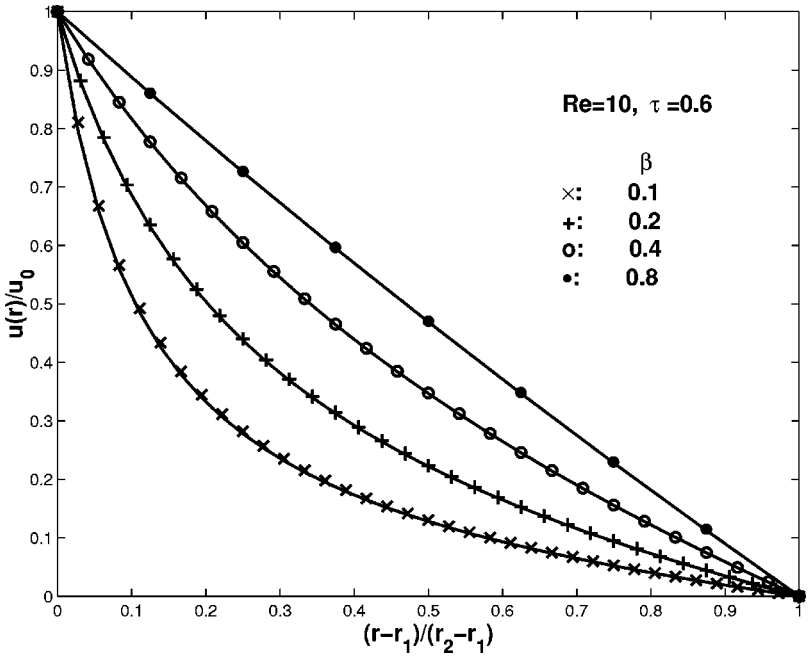

FIG. 2. Velocity profiles of the Couette flow at Re $=10$ with different values of the radius ratio.

To demonstrate the different behaviors of the two treatments, a fully developed two-dimensional steady Poiseuille flow is considered. The Reynolds number of the Poiseuille flow is defined by $\mathrm{Re}=Hu_0/\nu$, where $u_0=FH^2/(8\rho_0\nu)$ is the peak velocity, F is the driven force, $H=(N_y-3+2\Delta)$ is the channel height. Here Δ is the distance between the upper (or bottom) wall and the nearest layer of fluid nodes. The driven force F is included by adding an additional term after the collision step, $f_i^+(\mathbf{x},t)=f_i^+(\mathbf{x},t)+\omega_i F\mathbf{e}_{ix}/c_s^2$. Since the MLS scheme has better numerical stability than the FH scheme, we only make comparisons between the present and the MLS treatments. In simulations u_0 is set to be 0.1 in all cases, and a lattice with $N_y\times N_x=35\times 33$ nodes is used. Periodic boundary condition is applied to the inlet and exit, and the boundary condition for f_i on the top and bottom walls is implemented following the MLS or the present treatment.

The MLS treatment encounters no numerical instability for $\Delta\geqslant 0.5$. But for $\Delta<0.5$, numerical instability appears, and τ must be smaller than 2.0. For the present treatment, the computation is stable for a large range of τ and Δ, and the steady (τ,Δ) region covers that of the MLS treatment. In fact, the computation is still stable even as $\tau=100$ for $0\leqslant\Delta\leqslant 1$, although the solution deviates from the analytical solution. $\tau_{\min}$, the minimum value of τ at which the computation is stable for a given Δ, is also compared between the present and the MLS treatments. It is found that for $\Delta=0.1$, $\tau_{\min}=0.509$ $(\mathrm{Re}=1073.33)$ for the MLS treatment, and 0.506 $(\mathrm{Re}=1610)$ for the present treatment. For $\Delta=0.2$, $\tau_{\min}=0.505$ $(\mathrm{Re}=1.944\times 10^3)$ for the MLS treatment, and 0.500 03 $(\mathrm{Re}=3.24\times 10^5)$ for the present treatment. For $\Delta\geqslant 0.3$ it is found the computations are still stable for both treatments even as $\tau-0.5=10^{-7}$, and for every

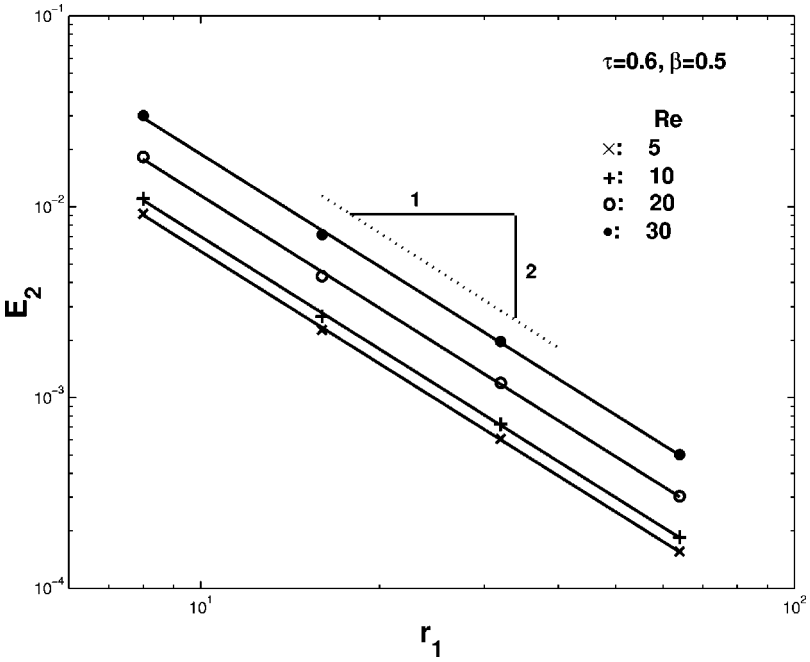

FIG. 3. Relative global errors versus the radius of the inner cylinder in the Couette flow. Solid lines are the least-square fittings.

value of τ at which the MLS scheme is stable, the present scheme is also stable. These facts indicate that the present treatment has better numerical stability than the MLS one.

To demonstrate the capability of the present boundary condition treatment for complex geometries, the Couette flow between two circular cylinders is also simulated. In this flow, the inner cylinder with radius r_1 rotates with a constant angular velocity ω and the outer cylinder with radius r_2 is kept stationary. This Couette flow has the following analytical solution

$$u_\theta(r) = \frac{u_0 \beta}{1-\beta^2}\left(\frac{r_2}{r} - \frac{r}{r_2}\right),$$

where $u_0 = \omega r_1$ and $\beta = r_1/r_2$.

In simulations, a square mesh is used to cover the flow domain. The present boundary treatment is then applied to the surfaces of the outer and inner cylinders. Numerical simulations for different values of β are first conducted to demonstrate the reliability of the present boundary treatment. We use $\tau = 0.6$, $r_2 = 80$, and r_1 changes according to r_2 and β. The Reynolds number of the flow, $\mathrm{Re} = (r_2 - r_1)u_0/\upsilon$, is kept at 10. The velocity profiles are plotted together with the analytical ones in Fig. 2. One can see that the agreement between the LBM and the analytical solutions is excellent.

Convergence rate of the treatment is also tested for different values of Re. In simulations, we use $\tau = 0.6$ and $\beta = 0.5$. r_1 changes from 8 to 64, and r_2 changes according to β and r_1. The relative global L_2 norm errors in the velocity filed E_2 are measured and shown in Fig. 3. Asymptotical quadratic convergence is clearly observed from the figure, and the second-order accuracy of the treatment for curved walls is confirmed.

In summary, a new treatment for curved boundary in the lattice Boltzmann method has been proposed based on the idea of extrapolation of the nonequilibrium. The treatment is of second-order accuracy. Numerical results indicate that the present treatment can preserve the accuracy of the geometry of the physical boundaries. It is also found that the proposed treatment exhibits better numerical stability compared with two previous treatments for curved boundaries. With these attractive features, the present boundary treatment is expected to make a substantial contribution to LBM for simulating practical fluid flows.

ACKNOWLEDGMENTS

Z.G. would like to thank Professor Y. H. Qian and Professor H. P. Fang for helpful discussions. He also sincerely thanks Professor L.-S. Luo for his helpful suggestions. This work is subsidized by the Special Funds for Major State Basic Research Projects (G1999022207) and the National Natural Science Foundation (60073044).

[1] S. Chen and G. Doolen, "Lattice Boltzmann method for fluid flows," Annu. Rev. Fluid Mech. **30**, 329 (1998).
[2] R. Cornubert, D. d'Humeiéres, and D. Levermore, "A Knudsen layer theory for lattice gases," Physica D **47**, 241 (1991).
[3] D. R. Noble, S. Chen, J. G. Georgiadis, and R. O. Buckius, "A consistent hydrodynamic boundary condition for the lattice Boltzmann method," Phys. Fluids **7**, 203 (1995).
[4] D. P. Ziegler, "Boundary conditions for lattice Boltzmann simulations," J. Stat. Phys. **71**, 1171 (1993).
[5] Q. Zou, and X. He, "On pressure and velocity boundary conditions for the lattice Boltzmann BGK model," Phys. Fluids **9**, 1591 (1997).
[6] S. Chen, D. Martinez, and R. Mei, "On boundary conditions in lattice Boltzmann methods," Phys. Fluids **8**, 2527 (1996).
[7] O. Filippova and D. Hänel, "Grid refinement for lattice-BGK models," J. Comput. Phys. **147**, 219 (1998).
[8] R. Mei, L-S. Luo, and W. Shyy, "An accurate curved boundary treatment in the lattice Boltzmann method," J. Comput. Phys. **155**, 307 (1999).
[9] X. He and L.-S. Luo, "Lattice Boltzmann model for the incompressible Navier–Stokes equation," J. Stat. Phys. **88**, 927 (1997).
[10] J. D. Sterling and S. Chen, "Stability analysis of the lattice-Boltzmann methods," J. Comput. Phys. **123**, 196 (1996).